Structures 47 (2023) 233–245

Contents lists available at ScienceDirect

Structures

journal homepage: www.elsevier.com/locate/structures

Development of Non-sticking Steady-State solution for structures with hybrid damping mechanism

Mohammad Ziaee [a], Farzad Hejazi [b,*]

[a] Department of Civil Engineering, University Putra Malaysia, Malaysia
[b] Faculty of Environment and Technology, The University of The West England, Bristol, UK

ARTICLE INFO

Keywords:
Vibration
Dynamic Load
Coulomb Friction
Viscous Damper
Hybrid Damping
Energy Dissipation System
Structural Response

ABSTRACT

Energy dissipation occurs through Coulomb friction and is considered a conventional type of mechanical damping mechanism in structures subjected to external loads. Structures that are subjected to severe dynamic excitations such as ground motion or wind are required to employ a supplementary dampening system in addition to the Coulomb damping to mitigate the adverse impact of vibration in structures.

Therefore, this study aims to develop a new Hybrid Damping Mechanism (HDM) for a single-degree-of-freedom (SDOF) system which is subjected to harmonic loads through a Viscous Damper System (VDS) to enhance the energy dissipation efficiency besides the Coulomb friction. Therefore, an analytical dynamic model for the non-sticking steady-state response was formulated where the effects of the viscous damper were implemented in the governor equation of the motion to estimate the structural response under harmonic loads. Subsequently, the Maximum Displacement (MD) and the Maximum Velocity (MV) were estimated by assuming deviation from the equilibrium point. Finally, a genuine borderline equation and a boundary limit were derived for the force amplitude ratio, where the maximum external load was divided by kinetic friction. It is an appropriate guideline for structural designers to avoid the sticking phase in the dynamical analysis of the structural systems equipped with frictional dampers.

Based on the application of the final solution to a numerical example, the proposed HDM in the SDOF system considerably diminished the MD with velocity deviation ranging between 5% and 98% and 3% to 94%, respectively. Meanwhile, the analysis also revealed that the VDS damping ratio and the force amplitude ratio were the most effective parameters in reducing the MD and velocity deviation with a frequency ratio (β) between 0.85 and 1.15.

The developed hybridized SDOF system can also be applied as a Tuned Mass Damper (TMD) in the structures to ameliorate their dynamic response.

1. Introduction

Friction could occur in various conditions to resist the movement of one object over another in sliding or rolling motions [1]. For instance, friction is the main cause of the dissipation of energy in industrial machinery or structures where the components have relative motions [2]. Energy dissipation in structures occurs through material friction, friction between structural components, and damage or yielding in structural members. However, supplementary structural vibration dampening systems such as frictional dampers were implemented in a structure subjected to catastrophic excitation to enhance the efficiency of energy dissipation in the past decades [3]. The base isolators are deemed as alternative solutions to decouple the superstructure from its substructure to isolate it and dissipate the effects of applied ground motion [4]. The different types of isolation systems developed include rubber bearings, friction bearings, and spring bearings. Friction forces can play a pivotal role in stabilizing the responses of dynamic systems based on the type of damping or isolating systems used. Therefore, its effects on dynamic systems must be investigated in detail.

Harmonic motion includes the intermittent transformation of energy between potential and kinetic forms. During this energy conversion, the energy loss occurs in each cycle based on whether the dynamic system is equipped with dampers [5]. Even though the conventional dampening devices are mostly passive systems, the semi-active approaches are

* Corresponding author.
E-mail address: farzad.hejazi@uwe.ac.uk (F. Hejazi).

https://doi.org/10.1016/j.istruc.2022.10.118
Received 12 May 2022; Received in revised form 8 September 2022; Accepted 26 October 2022

employed in some special cases a change in the performance of the control system is required according to the applied loads [6]. For instance, when the effectiveness of the TMD downgrades due to detuning, an external force is applied to TMD or directly to the main structure to maintain the efficiency of the damping device in energy dissipation. Therefore, this system is considered a Semi-Active Tuned Mass Damper (SATMD). However, the structural response under applied dynamic loads needs to be determined to calculate the total amount of energy dissipation for any type of dampening system (passive or semi-active).

In structures subjected to an external load, the Coulomb friction causes energy dissipation in the structure. As the main focus in back-and-forth motions in presence of the friction force is preventing the sticking phase, Den Hartog [7] proposed a non-sticking steady-state solution for the single-degree-of-freedom (SDOF) systems with friction subjected to harmonic loads in 1931. Hartog's derivations [7] were intended for the non-sticking phase and possessed some basic postulations such as the maximum velocity (MV) at a static equilibrium point. However, an alternative solution for the sticking and sliding phases effects was suggested by Hong et al. in 2000 [8]. Meanwhile, Hundal (1979) determined the response of the SDOF system with Coulomb friction and viscous damping, subjected to base excitation [9]. Whereas, Beucke et al. [10] worked on a dynamic model which was the combination of VDS, constant Coulomb friction, and linear Coulomb friction. Although the authors proposed a steady-state solution to predict the structural responses, the results did not include maximum displacement (MD) and MV which are considered important parameters in structural design.

More research was carried out to determine the steady-state response of the structures furnished with conventional damping systems using various mathematical-based techniques. The time-domain numerical integration method was used for the analysis of the steady-state motion of an SDOF Coulomb oscillator equipped with a viscous damper system with multiple stops per cycle [11]. In another study, the frequency domain analysis of frictional damped systems with the aid of the incremental harmonic balance method was performed to derive the steady-state response of the considered system [12]. The phase plane methods were also applied to SDOF systems with hysteresis dampers [13] to evaluate the dynamic behavior of the system and explore the structural responses. Furthermore, Nayfeh et al. [14] employed the Equivalent Linearization Method (ELM) to determine the response of the dynamic system. In 2021, Cacciola et al. developed the Preisach formalism method to model the mechanical behavior of soil and estimated the steady-state response of the nonlinear soil-structure interaction problems [15]. In a different study, a numerical method of Hysteresis Identification via Reversal Points (HIRP) was proposed to calculate the steady-state response of frictional nonlinear systems under harmonic loads [16]. While a recent study [17] evaluated the response of an SDOF system with Coulomb damping subjected to harmonic base excitation based on Hartog's equation [7].

Furthermore, the steady-state response of the multi-degree-of-freedom (MDOF) system with the Coulomb friction contact under harmonic loading was investigated by Marino et al. [18]. Yadav et al. [19] also applied Den Hartog's [7] equation for a mechanical problem and extended it numerically to determine the stick–slips and jerks in the SDOF system with dry friction and clearance. A steady-state solution for lightly damped MDOF systems in contact with Coulomb friction was derived and formulated by Marino et al. [20]. This method is applicable and limited only to light-damped structures as it is not capable of formulating MV, deviation points, and time lag. Therefore, there is a lack of valid results for moderate and heavy damped structures (structures with a hybrid damping system) with Coulomb friction. Comparatively, amongst the numerous proposed steady-state solutions, Hartog's method was simple and is an easy process equation frequently used by numerous researchers. However, the main drawbacks of this solution revealed by Hong et al. [3] included the inability to estimate the MV, its deviation from the static equilibrium point, and its corresponding time lag.

Based on the aforementioned discussion, prior studies mainly focused on SDOF systems with the Coulomb friction subjected to an external load. Since the investigated systems were ineffective under severe excitations, this study employed the VDS as a supplementary damping mechanism besides the Coulomb friction to enhance the energy dissipation efficiency. For this purpose, new equations for the non-sticking steady-state response of the proposed Hybrid Damping System (HDS) were formulated. Also, an equation for the force amplitude ratio is proposed which is applicable as a design guideline for the structural engineers to skip the sticking phase in their calculations.

2. Development of HDS

Generally, energy dissipation in a structure occurs through material friction, elements friction or structural damage. Since the inherent friction is not adequate to dissipate the energy in the structures subjected to severe excitations, it is necessary to enhance the energy dissipation efficiency to protect structures against applied vibration.

To address this issue, HDS is proposed in this study through the application of VDS together with the Coulomb friction mechanism. Thus, the effects of VDS implemented in the governor equation of motion of an SDOF system and the structural responses under harmonic load were used to evaluate the effectiveness of the proposed system. The proposed hybridized damping mechanism for the SDOF system is also applicable in structures such as Tuned Mass Damper.

The schematic model of the proposed HDS for SDOF is depicted in Fig. 1. Where m denotes the mass of the system, c is the viscous damping coefficient, k refers to the stiffness of mass-less spring, x is the displacement, $\dot{x}$ and $\ddot{x}$ are the velocity and acceleration, respectively (the first and second derivatives of displacement to time), P_0 and ω_f designate the amplitude and frequency of external loading, respectively, and t the elapsed time. Also, to consider the effect of friction in the mass-spring-damper system, it is assumed that the mass is moving over a rough horizontal surface. Whereby, f_d is the frictional force, N is the gravity force due to the weight of the lumped mass which is applied in a perpendicular direction of movement, and μ_k is kinetic friction coefficient.

The governing equation of motion for the considered SDOF structure with an HDS can be formulated through the equilibrium equation:

$$m\ddot{x} + c\dot{x} + kx = P_0 sin\omega_f t - r_a \tag{1}$$

Where r_a is the friction force due to the Coulomb friction generated in the opposite direction of friction.

The constitutive force can then be formulated through the summation of the spring and friction forces:

$$r = r_b + r_a \tag{2}$$

In where;

$$r_b = kx, |r_a| \le f_d \tag{3}$$

As mentioned before, μ_k is referred to as the kinetic friction coefficient which is dependent on the type of contacting material as expressed in Table 1 for the main construction materials including concrete, steel and wood. These details were obtained empirically.

To formulate the response of the considered SDOF with an HDS under harmonic loads, a steady-state non-sticking cycle of motion was considered, where the phase curve of the motion in the phase plane (x, $\dot{x}$) is assumed to be symmetrical (Fig. 2).

In Fig. 2, Δ_0 and V_0 designate the MD and velocity, respectively. Also, it is assumed that the points of the maximum and minimum velocities are not located on the $\dot{x}$ axis, so, the two points were let to deviate from the $\dot{x}$ axis with an unknown deviation Δ_1.

In the SDOF system subjected to external loads, the MV occurs at a static equilibrium point. However, when an external load is removed

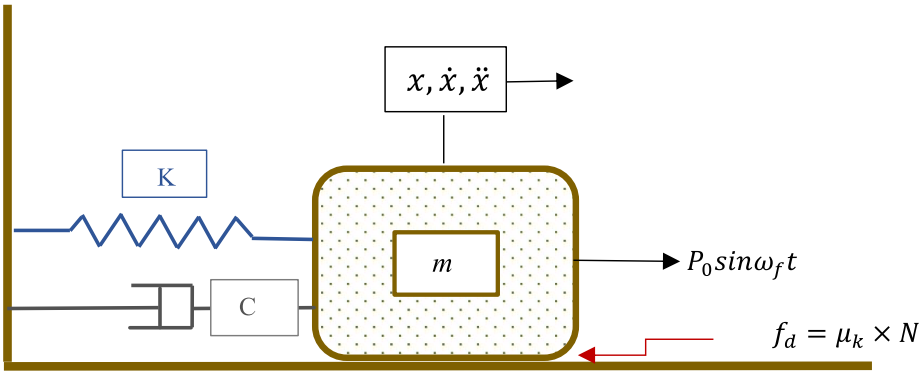

Fig. 1. Schematic model of the proposed hybrid system.

Table 1
Friction coefficient for different construction materials.

System	Static friction μ_s	Kinematic friction μ_k
Rubber on dry concrete	1	0.7
Rubber on wet concrete	0.7	0.5
Steel on steel (dry)	0.6	0.3
Steel on steel (oiled)	0.05	0.03
Metal on wood	0.5	0.3

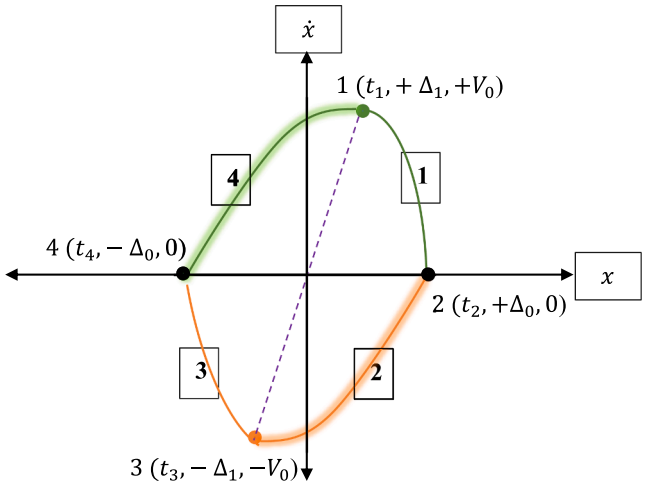

Fig. 2. The assumed in phase plane curve for non-sticking movement.

(unloaded), the damping mechanism dissipates the energy and consequently, the mass rests at the static equilibrium point ($kx_e = mg$). Therefore, the MV and rest points will be the same.

When Coulomb friction is applied to the oscillatory system, the mass stops at a distance from the static equilibrium point due to friction force that resists the returning mass to its static equilibrium point. The point at which the mass stops is called the pseudo-static equilibrium point ($kx_{se} + f_d = mg$). Therefore, similar to a static equilibrium point, it can be postulated that the MV in presence of the Coulomb friction force occurs at the pseudo-static equilibrium point ($\Delta_1 = x_e - x_{se}$).

Therefore, the x and $\dot{x}$ for different times are expressed as the following coordinates:

$$(x(t_1), \dot{x}(t_1)) = (+\Delta_1, +V_0), (x(t_2), \dot{x}(t_2)) = (+\Delta_0, 0)(x(t_3), \dot{x}(t_3)) = (-\Delta_1, -V_0), \quad (x(t_4), \dot{x}(t_4)) = (-\Delta_0, 0) \tag{4}$$

Where the time intervals are interlaced by the following equations:

$$t_3 = t_1 + \pi/\omega_f t_4 = t_2 + \pi/\omega_f \tag{5}$$

Since the phase curve has a closed form, formulations would be done only for one-half of the curve either the right or left branch [15]. If the upper or lower branches are considered, the analytic method would be similar to that of Hartog's [1]. This state of affairs deals with both upper and right branches solves the differential governing equation of the motion in two different phases, and finally proposes the possible solution for the steady-state response of hybridized SDOF system. Although the solution for the governor equation of motion was expected to be similar to that of Hong et al. [15], nuanced discrepancies were observed between Hong et al.'s solution and the proposed solution attributable to the implementation of VDS in the SDOF system.

2.1. Formulation of the steady-state response for the right branch

In this case, the formulation of the steady-state response is done by considering the right branch of Fig. 2. For the time interval of $t_1 \le t \le t_2$ (part 1 in Fig. 2), the steady-state solution for clockwise direction would be in the form of:

$$x_1(t) = Asin\omega_f t - B + e^{-\xi\omega_n(t-t_1)}(a_1 sin\omega_d(t-t_1) + b_1 cos\omega_d(t-t_1)) \tag{6}$$

Here,

$$A = \frac{P_0}{k\sqrt{(1-\beta^2)^2 + (2\xi\beta)^2}}, B = \frac{A\sqrt{(1-\beta^2)^2 + (2\xi\beta)^2}}{\alpha}, \alpha = \frac{P_0}{+f_d} \tag{7}$$

$$\beta = \frac{\omega_f}{\omega_n}, \omega_n = \sqrt{\frac{k}{m}}, \omega_d = \omega_n\sqrt{1-\xi^2}, \xi = 2m\omega_n \tag{8}$$

In which, α is the force amplitude ratio, B the static displacement due to the friction force where the mass sustains sufficient spring force to overcome the friction, β is the frequency ratio, ω_f is the frequency of the external loading, ω_n is the natural frequency of the structure, ω_d is the frequency of the damped system, ξ indicates the hybrid damping ratio which is the summation of inherent damping and supplementary viscous damping system, t is time, t_1 is the time at which the maximum positive velocity occurs, and a_1 and b_1 are constants. The idea was to designate various parameters similar to that of Hong et al. [15] for comparison purposes. As for the time interval of $t_2 \le t \le t_3$ (part 2 in Fig. 2), the steady-state solution in an anti-clockwise direction was expanded as:

$$x_2(t) = Asin\omega_f t + B + e^{+\xi\omega_n(t_3-t)}(a_2 sin\omega_d(t_3-t) + b_2 cos\omega_d(t_3-t)) \tag{9}$$

In which a_2 and b_2 are constants. The power of exponential is positive as the anti-clockwise direction is considered. If time (t) is changed with the time needed to reach the maximum negative velocity (t_3) in Eqn. (9) and the time required to reach the maximum negative velocity (t_3) is replaced by the time at which the maximum positive velocity happens (t_1), the Eqn. (6) must be gained. These mathematical tricks provide the opportunity to cast the steady-state response of the motion for clockwise

and anti-clockwise directions in a symmetrical way. To tackle the problem, it is necessary to obtain the first and second derivatives of displacement concerning time. Therefore, the velocity and acceleration can be expressed as:

$$\dot{x}_1(t) = A\omega_f cos\omega_f t + e^{-\xi\omega_n(t-t_1)}(a_1\omega_d cos\omega_d(t-t_1) - b_1\omega_d sin\omega_d(t-t_1)) - \xi\omega_n e^{-\xi\omega_n(t-t_1)}(a_1 sin\omega_d(t-t_1) + b_1 cos\omega_d(t-t_1)) \quad (10)$$

$$)\overline{t_1 \le t \le t_2}$$

$$\ddot{x}_1(t) = -A\omega_f{}^2 sin\omega_f t + e^{-\xi\omega_n(t-t_1)}\left(-a_1\omega_d{}^2 sin\omega_d(t-t_1) - b_1\omega_d{}^2 cos\omega_n(t-t_1)\right) - \xi\omega_n e^{-\xi\omega_n(t-t_1)}(a_1\omega_d cos\omega_d(t-t_1) - b_1\omega_d sin\omega_d(t-t_1)) - \xi\omega_n e^{-\xi\omega_n(t-t_1)}(a_1\omega_d cos\omega_d(t-t_1) - b_1\omega_d sin\omega_d(t-t_1)) + (\xi\omega_n)^2 e^{-\xi\omega_n(t-t_1)}(a_1 sin\omega_d(t-t_1) + b_1 cos\omega_d(t-t_1)) \quad (11)$$

$$)\overline{t_1 \le t \le t_2}$$

$$\dot{x}_2(t) = A\omega_f cos\omega_f t + e^{+\xi\omega_n(t_3-t)}(-a_2\omega_d cos\omega_d(t_3-t) + b_2\omega_d sin\omega_d(t_3-t)) - \xi\omega_n e^{-\xi\omega_n(t_3-t)}(a_2 sin\omega_d(t_3-t) + b_2 cos\omega_d(t_3-t)) \quad (12)$$

$$)\overline{t_2 \le t \le t_3}$$

$$\ddot{x}_2(t) = -A\omega_f{}^2 sin\omega_f t + e^{+\xi\omega_n(t_3-t)}\left(-a_2\omega_d{}^2 sin\omega_d(t_3-t) - b_2\omega_d{}^2 cos\omega_n(t_3-t)\right) - \xi\omega_n e^{+\xi\omega_n(t_3-t)}(-a_2\omega_d cos\omega_d(t_3-t) + b_2\omega_d sin\omega_d(t_3-t)) - \xi\omega_n e^{+\xi\omega_n(t_3-t)}(-a_2\omega_d cos\omega_d(t_3-t) + b_2\omega_d sin\omega_d(t_3-t)) + (\xi\omega_n)^2 e^{+\xi\omega_n(t_3-t)}(a_2 sin\omega_d(t_3-t) + b_2 cos\omega_d(t_3-t)) \quad (13)$$

$$)\overline{t_2 \le t \le t_3}$$

By considering the underlaid conditions (Eqs. (14) to (16)), the initial conditions at time t_2 must satisfy both of the proposed steady-state solutions (Eqs. (6) and (9) simultaneously), and hypothesizing new assumptions (Eqn. (17)), 10 equations with nine unknowns would be obtained. To achieve acceptable results, one of the equations must be satisfied with the results of the other nine equations.

Thus, solving the nine selective equations simultaneously results in the motion parameters. The procedure can be explained as:

$$x_1(t_1) = +\Delta_1, x_1(t_2) = +\Delta_0, x_2(t_2) = +\Delta_0, x_2(t_3) = -\Delta_0 \quad (14)$$

$$\dot{x}_1(t_1) = +V_0, \dot{x}_1(t_2) = 0, \dot{x}_2(t_2) = 0, \dot{x}_2(t_3) = -V_0 \quad (15)$$

$$\ddot{x}_1(t_1) = 0, \ddot{x}_2(t_3) = 0, \quad (16)$$

As $\xi \ll 1$, then $\xi^2 \cong 0$. So, it can be revealed that:

$$\omega_n = \omega_d, \beta = \beta_d \rightarrow \frac{\omega_f}{\omega_n} = \frac{\omega_f}{\omega_d}, e^{+\xi\omega_n(t_3-t_2)} \cong e^{-\xi\omega_n(t_2-t_1)} \quad (17)$$

By applying the initial conditions to the Eqs. (6), (9), and (10) through (13) and substituting the following statement, $t_3 = t_1 + \pi/\omega_f$, in the Eqs. (14), (15), and (16), the final 10 equations emerge as what follows:

$$)\overline{1} \rightarrow x_1(t_1) = Asin\omega_f t_1 - B + b_1 = +\Delta_1 \quad (18)$$

$$)\overline{2} \rightarrow x_1(t_2) = Asin\omega_f t_2 - B + e^{-\xi\omega_n(t_2-t_1)}(a_1 sin\omega_n(t_2-t_1) + b_1 cos\omega_n(t_2-t_1)) = +\Delta_0 \quad (19)$$

$$)\overline{3} \rightarrow x_2(t_2) = Asin\omega_f t_2 + B + e^{-\xi\omega_n(t_2-t_1)}\left(-a_2 sin\omega_n\left(t_2 - t_1 - \frac{\pi}{\omega_f}\right) + b_2 cos\omega_n\left(t_2 - t_1 + \frac{\pi}{\omega_f}\right)\right) = +\Delta_0 \quad (20)$$

$$)\overline{4} \rightarrow x_2(t_3) = -Asin\omega_f t_1 + B + b_2 = -\Delta_1 \quad (21)$$

$$)\overline{5} \rightarrow \dot{x}_1(t_1) = A\omega_f cos\omega_f t_1 + a_1\omega_n - \xi\omega_n b_1 = +V_0 \quad (22)$$

$$)\overline{6} \rightarrow \dot{x}_1(t_2) = A\omega_f cos\omega_f t_2 + e^{-\xi\omega_n(t_2-t_1)}(a_1\omega_n cos\omega_n(t_2-t_1) - b_1\omega_n sin\omega_n(t_2-t_1)) - \xi\omega_n e^{-\xi\omega_n(t_2-t_1)}(a_1 sin\omega_n(t_2-t_1) + b_1 cos\omega_n(t_2-t_1)) = 0 \quad (23)$$

$$)\overline{7} \rightarrow \dot{x}_2(t_2) = A\omega_f cos\omega_f t_2 + e^{-\xi\omega_n(t_2-t_1)}\left(-a_2\omega_n cos\omega_n\left(t_2 - t_1 + \frac{\pi}{\omega_f}\right) - b_2\omega_n sin\omega_n\left(t_2 - t_1 + \frac{\pi}{\omega_f}\right)\right) - \xi\omega_n e^{-\xi\omega_n(t_2-t_1)}\left(-a_2 sin\omega_n\left(t_2 - t_1 + \frac{\pi}{\omega_f}\right) + b_2 cos\omega_n\left(t_2 - t_1 + \frac{\pi}{\omega_f}\right)\right) = 0 \quad (24)$$

$$)\overline{8} \rightarrow \dot{x}_2(t_3) = -A\omega_f cos\omega_f t_1 - a_2\omega_n - \xi\omega_n b_2 = -V_0 \quad (25)$$

$$)\overline{9} \rightarrow \ddot{x}_1(t_1) = -A\omega_f{}^2 sin\omega_f t_1 - b_1\omega_n{}^2 - \xi\omega_n{}^2 a_1 - \xi\omega_n{}^2 a_1 = 0 \quad (26)$$

$$)\overline{10} \rightarrow \ddot{x}_2(t_3) = +A\omega_f{}^2 sin\omega_f t_1 - b_2\omega_n{}^2 + \xi\omega_n{}^2 a_2 + \xi\omega_n{}^2 a_2 = 0 \quad (27)$$

2.2. Formulation of the steady-state response for the upper branch

Finding the steady-state response for the upper branch requires some mathematical measures. In this case, the reference point to reshape the steady-state solution of the motion is the time at point 1 (t_1). Hence, the clockwise direction x_1 was used. It is assumed that the oscillatory motion begins from point 4 where $t_4 + \pi/\omega_f = t_2$. Thus, for the time interval of $t_4 \le t \le t_2$ (parts 4 and 1 in Fig. 2), the equation of motion takes the form of:

$$x_1(t) = Asin\omega_f t - B + e^{-\xi\omega_n(t-t_1)}(a_1 sin\omega_d(t-t_1) + b_1 cos\omega_d(t-t_1)) \quad (28)$$

$$)\overline{t_4 \le t \le t_2}$$

The parameters were determined through the Eqs. (7) to (8), where a_1 and b_1 are constants. It is also necessary to re-obtain the velocity and acceleration equations as the first and second derivatives of the displacement regarding time to further the formulation. So, by considering the first and second derivatives of Eqn. (28) for the time it is observed that velocity and acceleration take the following forms:

$$\dot{x}_1(t) = A\omega_f cos\omega_f t + e^{-\xi\omega_n(t-t_1)}(a_1\omega_d cos\omega_d(t-t_1) - b_1\omega_d sin\omega_d(t-t_1)) - \xi\omega_n e^{-\xi\omega_n(t-t_1)}(a_1 sin\omega_d(t-t_1) + b_1 cos\omega_d(t-t_1)) \quad (29)$$

$$)\overline{t_4 \le t \le t_2}$$

$$\ddot{x}_1(t) = -A\omega_f{}^2 sin\omega_f t + e^{-\xi\omega_n(t-t_1)}\left(-a_1\omega_d{}^2 sin\omega_d(t-t_1) - b_1\omega_d{}^2 cos\omega_n(t-t_1)\right) - \xi\omega_n e^{-\xi\omega_n(t-t_1)}(a_1\omega_d cos\omega_d(t-t_1) - b_1\omega_d sin\omega_d(t-t_1)) - \xi\omega_n e^{-\xi\omega_n(t-t_1)}(a_1\omega_d cos\omega_d(t-t_1) - b_1\omega_d sin\omega_d(t-t_1)) + (\xi\omega_n)^2 e^{-\xi\omega_n(t-t_1)}(a_1 sin\omega_d(t-t_1) + b_1 cos\omega_d(t-t_1)) \quad (30)$$

$$)\overline{t_4 \le t \le t_2}$$

Then by considering the new conditions as:

$$x_1(t_1) = \Delta_1, x_1(t_2) = +\Delta_0, x_1(t_4) = -\Delta_0 \quad (31)$$

$$\dot{x}_1(t_1) = V_0, \dot{x}_1(t_2) = 0, \dot{x}_1(t_4) = 0 \quad (32)$$

$$\ddot{x}_1(t_1) = 0 \quad (33)$$

The response of the hybridized system to the initial conditions can be expressed as:

$$\overline{)1}\rightarrow x_1(t_2) = Asin\omega_f t_2 - B + e^{-\xi\omega_n(t_2-t_1)}(a_1 sin\omega_n(t_2-t_1) + b_1 cos\omega_n(t_2-t_1)) = +\Delta_0 \tag{34}$$

$$\overline{)2}\rightarrow \dot{x}_1(t_2) = A\omega_f cos\omega_f t_2 + e^{-\xi\omega_n(t_2-t_1)}(a_1\omega_n cos\omega_n(t_2-t_1) - b_1\omega_n sin\omega_n(t_2-t_1)) - \xi\omega_n e^{-\xi\omega_n(t_2-t_1)}(a_1 sin\omega_n(t_2-t_1) + b_1 cos\omega_n(t_2-t_1)) = 0 \tag{35}$$

$$\overline{)3}\rightarrow x_1(t_4) = -Asin\omega_f t_2 - B + e^{-\xi\left(\omega_n(t_2-t_1)-\frac{\pi}{\beta}\right)}\left(a_1 sin\left(\omega_n(t_2-t_1)-\frac{\pi}{\beta}\right) + b_1 cos\left(\omega_n(t_2-t_1)-\frac{\pi}{\beta}\right)\right) = -\Delta_0 \tag{36}$$

$$\overline{)4}\rightarrow \dot{x}_1(t_4) = -A\omega_f cos\omega_f t_2 + e^{-\xi\left(\omega_n(t_2-t_1)-\frac{\pi}{\beta}\right)}\left(a_1\omega_n cos\left(\omega_n(t_2-t_1)-\frac{\pi}{\beta}\right) - b_1\omega_n sin\left(\omega_n(t_2-t_1)-\frac{\pi}{\beta}\right)\right) - \xi\omega_n e^{-\xi\omega_n(t_2-t_1)}\left(a_1 sin\left(\omega_n(t_2-t_1)-\frac{\pi}{\beta}\right) + b_1 cos\left(\omega_n(t_2-t_1)-\frac{\pi}{\beta}\right)\right) = 0 \tag{37}$$

$$\overline{)5}\rightarrow x_1(t_1) = Asin\omega_f t_1 - B + b_1 = \Delta_1 \tag{38}$$

$$\overline{)6}\rightarrow \dot{x}_1(t_1) = A\omega_f cos\omega_f t_1 + a_1\omega_n - \xi\omega_n b_1 = V_0 \tag{39}$$

$$\overline{)7}\rightarrow \ddot{x}_1(t_1) = -A\omega_f{}^2 sin\omega_f t_1 - 2\xi\omega_n{}^2 a_1 - b_1\omega_n{}^2 = 0 \tag{40}$$

In short, the seven equations that were derived with seven unknown parameters are more efficient than the right branch formulations with ten equations.

3. Formulating the maximum displacement of the structure equipped with the developed hybrid damping mechanism

In this section, an MD was formulated for the system with SDOF HDM. Similar to the previous section, the equations were established for both the upper and right branches where the final results were compared.

3.1. Formulating the maximum displacement using the right branch equations

To determine MD, the prementioned equations (Eqs (17) to (18)) must be solved. Therefore, a simplified form of those equations was required as demonstrated step by step here.

Superposition of Eqn. (18) to Eqn. (21) and Eqn. (22) to Eqn. (25) entails the below equation:

$$b_1 = -b_2, a_1 = +a_2 \tag{41}$$

Taking $\pi_1 = \pi/\beta$, the superposition of Eqs. (19) with (20) through trigonometric functions, and employing the Eqn. (41), resulted in a new statement:

$$e^{-\xi\omega_n(t_2-t_1)}\left(a_1 sin\left(\frac{\pi_1}{2}\right)cos\left(\omega_n(t_2-t_1)-\frac{\pi_1}{2}\right) - b_1 sin\left(\frac{\pi_1}{2}\right)sin\left(\omega_n(t_2-t_1)-\frac{\pi_1}{2}\right)\right) = +\Delta_0 - Asin\omega_f t_2 \tag{42}$$

Thereafter, Eqn. (19) was subtracted from the Eqn. (20) using the same assumption (i.e., $\pi_1 = \pi/\beta$):

$$e^{-\xi\omega_n(t_2-t_1)}\left(a_1 sin\left(\omega_n(t_2-t_1)-\frac{\pi_1}{2}\right) + b_1 cos\left(\omega_n(t_2-t_1)-\frac{\pi_1}{2}\right)\right)cos\left(\frac{\pi_1}{2}\right) = B \tag{43}$$

By combining the Eqs. (23) and (24), the following fundamental statement was obtained:

$$\frac{1}{\xi}\left(-a_1 sin\left(\omega_n(t_2-t_1)-\frac{\pi_1}{2}\right) - b_1 cos\left(\omega_n(t_2-t_1)-\frac{\pi_1}{2}\right)\right) - \left(a_1 cos\left(\omega_n(t_2-t_1)-\frac{\pi_1}{2}\right) - b_1 sin\left(\omega_n(t_2-t_1)-\frac{\pi_1}{2}\right)\right) = \frac{-A\beta sin\omega_f t_2}{\xi e^{-\xi\omega_n(t_2-t_1)}sin\left(\frac{\pi_1}{2}\right)} \tag{44}$$

Eqs. (43) and (44) are in the simplified form to simplify the other equations in this study. Next, the mathematical simplifications of deducting Eqn. (23) from the Eqn. (24) led to:

$$\frac{\left(a_1 cos\left(\omega_n(t_2-t_1)-\frac{\pi_1}{2}\right) - b_1 sin\left(\omega_n(t_2-t_1)-\frac{\pi_1}{2}\right)\right)}{\left(a_1 sin\left(\omega_n(t_2-t_1)-\frac{\pi_1}{2}\right) + b_1 cos\left(\omega_n(t_2-t_1)-\frac{\pi_1}{2}\right)\right)} = \xi \tag{45}$$

Combining Eqs. (42) to (45) and solving them simultaneously, yields the following formulas:

$$\overline{)cos\omega_f t_2} = \frac{(1+\xi^2)Bsin\pi_1}{A\beta(1+cos\pi_1)} \tag{46}$$

$$\overline{)sin\omega_f t_2} = \frac{\Delta_0}{A} - \frac{\xi Bsin\pi_1}{A(1+cos\pi_1)} \tag{47}$$

$$\overline{)t_2} = \frac{\pi}{2\omega_f} + \frac{1}{\omega_f}\left(arccos\left(\frac{\Delta_0}{A} - \frac{\xi Bsin\pi_1}{A(1+cos\pi_1)}\right)\right) \tag{48}$$

$$\overline{)\Delta_0} = \sqrt{A^2 - \left[\frac{(1+\xi^2)Bsin\pi_1}{\beta(1+cos\pi_1)}\right]^2} + \xi\left[\frac{Bsin\pi_1}{1+cos\pi_1}\right] \tag{49}$$

The Eqs. (46) to (49) represent the cosine and sine of the time lag for MD time to reach MD and the amount of MD, respectively. These parameters are the most important components of the developed hybridized SDOF system and can be compared with the result of the non-hybridized system reported by previous researchers.

3.2. Formulating the maximum displacement using the upper branch equations

In this section, Eqs. (34) to (40) were referred again to formulate MD using the upper branch equations. The same procedures demonstrated in the previous section for the right branch were employed by combining the equations from section 2.2 and simplifying the results to derive the following equations:

$$(34)+(36)\rightarrow \frac{cos\left(\frac{\pi_1}{2}\right)\left(a_1 sin\left(\omega_n(t_2-t_1)-\frac{\pi_1}{2}\right) + b_1 cos\left(\omega_n(t_2-t_1)-\frac{\pi_1}{2}\right)\right)}{B} = e^{\xi\omega_n(t_2-t_1)} \tag{50}$$

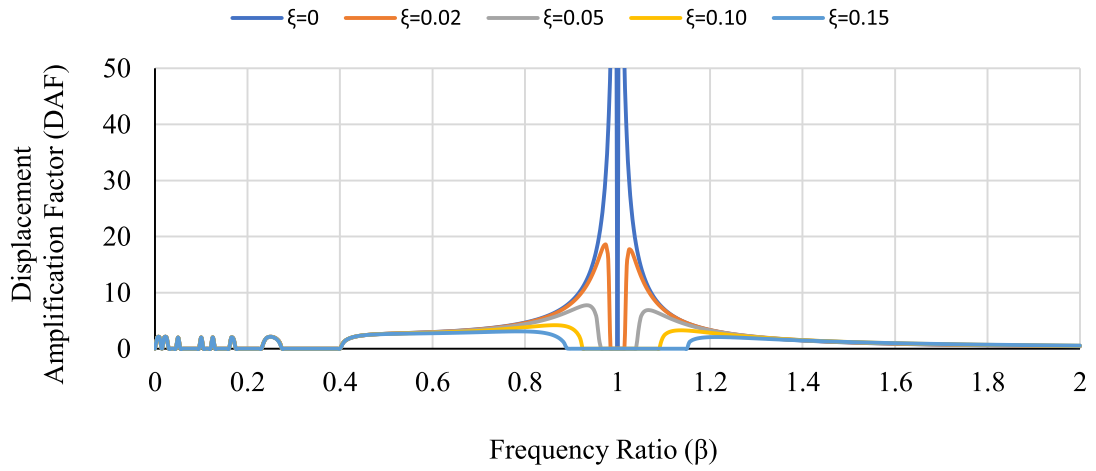

(a): Force amplitude ratio (α) = 2

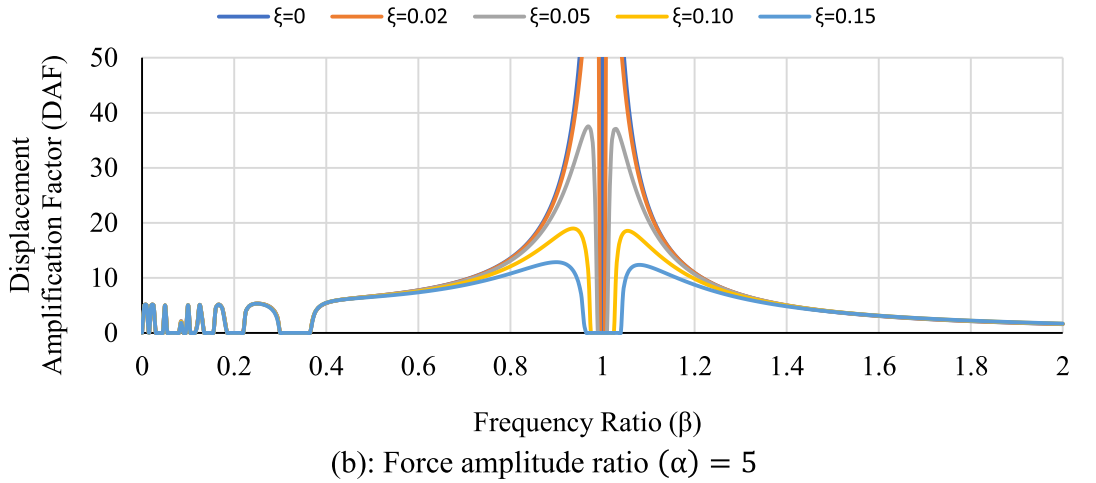

(b): Force amplitude ratio (α) = 5

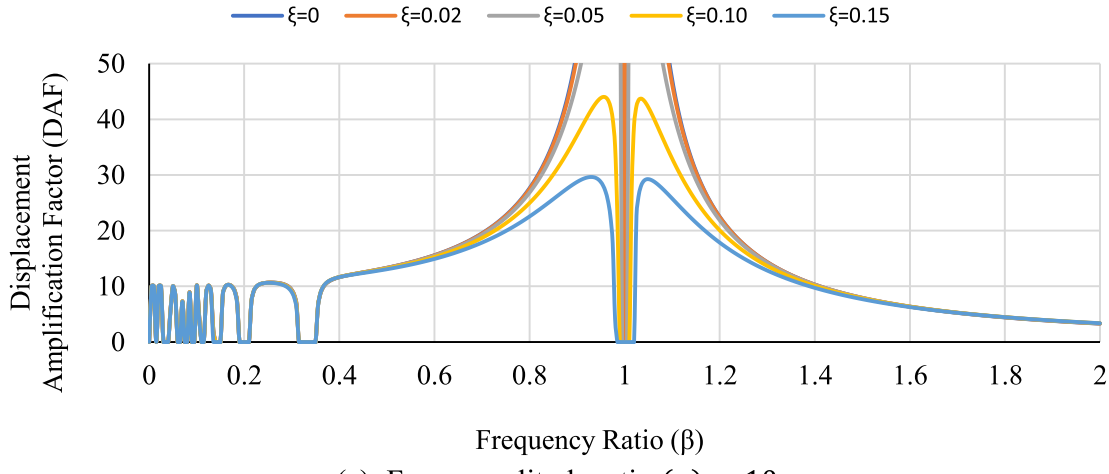

(c): Force amplitude ratio (α) = 10

Fig. 3. Displacement amplification factor (Δ_0/B) for SDOF with hybrid damping mechanism under harmonic load for various amounts of force amplitude ratio (α), frequency ratio (β) and hybrid damping ratio (ξ).

$$(34)-(36)\rightarrow e^{-\xi\omega_n(t_2-t_1)}\left(-a_1 sin\left(\frac{\pi_1}{2}\right)cos\left(\omega_n(t_2-t_1)-\frac{\pi_1}{2}\right)+b_1 sin\left(\frac{\pi_1}{2}\right)sin\left(\omega_n(t_2-t_1)-\frac{\pi_1}{2}\right)\right)+Asin\omega_f t_2=\Delta_0 \tag{51}$$

$$(35)+(37)\rightarrow tan\left(\omega_n(t_2-t_1)-\frac{\pi_1}{2}\right)=\frac{a_1-\xi b_1}{\xi a_1+b_1} \tag{52}$$

$$(35)-(37)\rightarrow e^{-\xi\omega_n(t_2-t_1)}sin\left(\frac{\pi_1}{2}\right)\left((\xi a_1+b_1)cos\left(\omega_n(t_2-t_1)-\frac{\pi_1}{2}\right)+(a_1-\xi b_1)sin\left(\omega_n(t_2-t_1)-\frac{\pi_1}{2}\right)\right)=A\beta cos\omega_f t_2 \tag{53}$$

Replacing Eqn. (50) into Eqn. (51) and introducing Eqn. (52) into it, brings about:

$$Asin\omega_f t_2+\xi Btan\left(\frac{\pi_1}{2}\right)=+\Delta_0 \tag{54}$$

and by re-arranging the considered equation, it can be obtained that:

$$)sin\omega_f t_2=\frac{\Delta_0}{A}-\frac{\xi Bsin\pi_1}{A(1+cos\pi_1)} \tag{55}$$

Solving Eqn. (54) for t_2 reveals that:

$$)t_2=\frac{\pi}{2\omega_f}+\frac{1}{\omega_f}\left(arccos\left(\frac{\Delta_0}{A}-\frac{\xi Bsin\pi_1}{A(1+cos\pi_1)}\right)\right) \tag{56}$$

Eqn. (56) is an important formula as it reveals that the time lag value is required to determine the MD. Replacing Eqn. (50) into Eqn. (34) plus the negative of Eqn. (37) and using the Eqn. (52) engenders another crucial equation regarding the hybrid system:

$$)cos\omega_f t_2=\frac{(1+\xi^2)Bsin\pi_1}{A\beta(1+cos\pi_1)} \tag{57}$$

Also, by combining Eqs. (54) and (57) it can be observed that:

$$)\Delta_0=\sqrt{A^2-\left[\frac{(1+\xi^2)Bsin\pi_1}{\beta(1+cos\pi_1)}\right]^2}+\xi\left[\frac{Bsin\pi_1}{1+cos\pi_1}\right] \tag{58}$$

or the Eqn. (58) in a dimensionless form, can be rearranged as:

$$)\frac{\Delta_0}{B}=\sqrt{\frac{\alpha^2}{(1-\beta^2)^2+(2\xi\beta)^2}-\left[\frac{(1+\xi^2)sin\pi_1}{\beta(1+cos\pi_1)}\right]^2}+\xi\left[\frac{sin\pi_1}{1+cos\pi_1}\right] \tag{59}$$

Eqn. (59) is regarded as Displacement Amplification Factor (DAF) for the SDOF with HDM under harmonic load. It is only dependent on three dimensionless parameters of force amplitude ratio (α), frequency ratio (β), and hybrid damping ratio (ξ). Based on the observation, the final equations obtained for the upper branch were similar to those derived for the right branch. Hence, the derivation throughout either branch relationship led to the same results.

3.3. Displacement amplification factor for SDOF with HDM

The MD described in Eqn. (58) was converted to a dimensionless form as DAF for SDOF system with HDM under harmonic load explained in Eqn. (59). Based on this equation, it is concluded that the ratio of MD of the SDOF with HDM subjected to harmonic load to the static displacement due to the friction force depends on a few dimensionless parameters including force amplitude ratio (α), frequency ratio (β), and hybrid damping ratio (ξ).

So, the variation of the DAF (Δ_0/B) regarding the force amplitude ratio (α), the frequency ratio (β), and damping ratio (ξ) were assessed by assuming a particular condition. By taking mass (m) $= 50,000kg$, friction force (f_d) $= 15,000N$ (considering the kinematic friction coefficient (μ_k) is almost close to oiled steel on steel friction as mentioned in Table 1), and the external force frequency (ω_f) $= 2\pi(rad/s)$, the corresponding graphs to DAF for the SDOF equipped with HDM under harmonic load for various amounts of force amplitude ratio (α), frequency ratio (β), and hybrid damping ratio (ξ) are depicted in Fig. 3. Based on these graphs, the variation of DAF for SDOF with HDM can be demonstrated in three ranges of frequency ratio (β) as described as follows:

i) Frequency ratio ($\boldsymbol{\beta}$)$\langle$0.6.

According to Fig. 3, the force amplitude ratio (α) is more effective in the variation of DAF compared to the hybrid damping ratio (ξ) with no effects in the lower range of β but the effects rose after $\beta = 0.6$. The DAF value was estimated at 2 in this range for the force amplitude ratio (α) of 2. However, by increasing α to 5 and 10, the DAF increased to 5 and 10, respectively. The results indicated that the DAF is equivalent to the force amplitude in the frequency ratio (β) of 0 to 0.6. DAF also increases when the force amplitude (α)is increased. Therefore, the fraction of external load amplitude divided by the Coulomb friction plays an important role in minimizing the DAF.

ii) 0.6 < Frequency ratio ($\boldsymbol{\beta}$)$\langle$1.15.

Referring to Fig. 3, both the force amplitude ratio (α) and the hybrid damping ratio (ξ) yielded significant effects on the DAF for frequency ratios of 0.6 to 1.15. Similar to the first range of frequency ratio, increasing the force amplitude ratio (α) increases the DAF. However, the hybrid damping ratio dissipates the displacement response due to the applied external harmonic load and increased hybrid damping ratio, thus reducing the DAF. In the close range of frequency ratio (β) equal to 1, the frequency of the external excitation is equal to the frequency of the structure. In this scenario, the resonance that occurs in the system and a minimum amount of damping prevents the extreme magnification of displacement response.

The minimum required damping ratio (ξ) depends on the force amplitude ratio (α), hence, DAF increases due to larger force amplitude ratios. For instance, the 2 % damping ratio leads to almost 18 DAFs for the force amplitude ratio of 2, however, to have the same DAF for frequency ratios of 5 and 10, the damping ratio of about 10 % and 25 % is required respectively. Although, DAF for 18 is noticeable high in the design of the structure, however by considering of low inherent damping for the structure which is 2 % for steel structures and 5 % for concrete structures, implementing a supplementary damping system to increase the overall damping of the system for higher force amplitude ratio is vital to avoid of catastrophic displacement response of structure during resonance range of β. To obtain an economic design (DAF equal or less than DAF in the range of β 0 to 0.6) in low force amplitude ratios (α equal or less than 2), a HDS is utilized to boost the overall damping of the system to up to 10 %.

Therefore, if the structure is not equipped with an HDM system with a frequency ratio (β) of 0.85 to 1.15, the structure will experience severe drifts. The back-and-forth displacements would lead to fatigue in the structural components, finally causing catastrophic structural damage and collapse. The results indicated that implementing the HDM in the above-mentioned SDOF system can considerably diminish DAF in the range of 5 % to 98 % for various frequency and force amplitude ratios.

iii) Frequency ratio ($\boldsymbol{\beta}$)$\rangle$1.15.

This range of frequency ratio (β) is the most appropriate zone to design the structures since the dynamic effects such as DAF are minimized by increasing the frequency ratio. This condition is obtained through a design process to make the natural frequency of the structure in a way that the frequency ratio (β) becomes greater than 1.15. However, in this zone increasing the hybrid damping ratio (ξ) may lead to the lower displacement amplitude, but the amount of deduction is not considerable in comparison to effect of increasing frequency ratio.

As it can be seen in all graphs, in the frequency ratio of 1.4 for any force amplitude ratio (α), DAF has the same amount as its constant values for the low-frequency ratio ($\beta = 0$ to 0.4). Also, by increasing the

frequency ratio beyond 1.4, DAF reduces. Therefore, the design of structure which lead to a higher frequency ratio ($\beta > 1.4$), results in lesser displacement amplitude. This method is considered as the economic design strategy since the dynamic load does not affect the response of the structure and the design for static forces is enough for resisting against imposed loads.

4. Deviation and time lag of maximum velocity for hybridized SDOF systems

This section focuses on the formulation of the MV of the proposed SDOF system with the HDM to derive the corresponding equation to determine the time required to reach the MV (t_1), the velocity deviation (Δ_1) and the MV (V_0).

Since the derivations from the upper or the right branch result in the same, only one derivation process is presented in this section.

4.1. Formulating maximum deviation of MV

To obtain MV, Eqn. (45) was recast by simplifying the enumerator and nominator as:

$$tan\left(\omega_n(t_2-t_1)-\frac{\pi_1}{2}\right)=\frac{a_1-\xi b_1}{\xi a_1+b_1} \tag{60}$$

By utilizing Eqn. (26) or Eqn. (40), the below statements can be originated from Eqn. (60):

$$\frac{a_1-\xi b_1}{\xi a_1+b_1}=\frac{a_1+2\xi^2 a_1+\xi A\beta^2 sin\omega_f t_1}{-A\beta^2 sin\omega_f t_1-\xi a_1}=f(a_1) \tag{61}$$

$$\frac{a_1-\xi b_1}{\xi a_1+b_1}=\frac{-b_1-2\xi^2 b_1-A\beta^2 sin\omega_f t_1}{\xi b_1-\xi A\beta^2 sin\omega_f t_1}=f(b_1) \tag{62}$$

Next, by multiplying the sides of Eqn. (61) to each other and simplifying it, the below equation arises:

$$-a_1 A\beta^2 sin\omega_f t_1-\xi^2 a_1 b_1=\xi^2 a_1 A\beta^2 sin\omega_f t_1+2\xi^3 {a_1}^2+a_1 b_1 \tag{63}$$

At this stage confronting the coefficients of "$sin\omega_f t_1$" in Eqn. (63) equal to each other, the following formula was generated:

$$\xi^2 a_1+a_1=0 \tag{64}$$

When the value from Eqn. (64) was replaced in Eqn. (62), a_1 and b_1 values were derived:

$$\overline{)a_1=0} \tag{65}$$

$$\overline{)b_1=-A\beta^2 sin\omega_f t_1} \tag{66}$$

The insertion of b_1 into Eqs. (18) or (38) yields:

$$sin\omega_f t_1=\frac{\sqrt{\left(1-\beta^2\right)^2+(2\xi\beta)^2}}{\left(1-\beta^2\right)}\times\frac{1}{\alpha}+\frac{\sqrt{\left(1-\beta^2\right)^2+(2\xi\beta)^2}}{\left(1-\beta^2\right)}\times\frac{k}{P_0}\times\Delta_1 \tag{67}$$

The following equation for MV with the understudied SDOF system and HDM can be derived using either Eqn. (22) or Eqn. (39) and introducing Eqs. (65) and (66):

$$\frac{V_0}{B\omega_f}=\sqrt{\frac{\alpha^2}{\left(1-\beta^2\right)^2+(2\xi\beta)^2}-\left(\left(\frac{1}{1-\beta^2}\right)\left(1+\frac{\Delta_1}{B}\right)\right)^2}+\xi\left(\frac{\beta}{1-\beta^2}\right)\left(1+\frac{\Delta_1}{B}\right) \tag{68}$$

Eqs. (67) and (68) are almost similar to the formulation reported by Hong et al. [15]. However, unlike the MD (Δ_0) and the time required for the MD to occur (t_2), the equations presented by Hong et al. [15] for the required time to reach the MV (t_1), the velocity deviation (Δ_1), and the MV (V_0) were not applicable for zero damping ratio (ξ). Due to the presence of the damping ratio as a coefficient in the velocity and acceleration equations of damped systems, the equations for the required time to reach the MV (t_1), the velocity deviation (Δ_1), and the MV (V_0), varied from the equations documented by Hong et al. [15].

However, regarding the displacement, this issue has not been affected and results of the undamped SDOF system are obtained from the equations corresponding to the damped systems by taking the damping ratio (ξ) equal to zero. It was highlighted that the time at point 1 (t_1) must be determined (as described in section 4.2) before estimating velocity deviation (Δ_1) and the MV (V_0) using Eqs. (67) and (68), respectively.

Based on the trigonometric relations, it is known that the value of the sine function lies within the range of (-1) to (+1). Thus, Eqn. (69) was derived by applying these boundary conditions to Eqn. (68):

$$-1\le\frac{\sqrt{\left(1-\beta^2\right)^2+(2\xi\beta)^2}}{\left(1-\beta^2\right)}\times\frac{1}{\alpha}+\frac{\sqrt{\left(1-\beta^2\right)^2+(2\xi\beta)^2}}{\left(1-\beta^2\right)}\times\frac{k}{P_0}\times(\Delta_1)\le+1 \tag{69}$$

Pre-multiplying Eqn. (69) to $\frac{(1+\beta^2)}{\sqrt{\left(1-\beta^2\right)^2+(2\xi\beta)^2}}\times\frac{P_0}{k}$ leads to:

$$-\frac{P_0}{k\alpha}-\frac{\left(1-\beta^2\right)}{\sqrt{\left(1-\beta^2\right)^2+(2\xi\beta)^2}}\times\frac{P_0}{k}\le\Delta_1\le\frac{\left(1-\beta^2\right)}{\sqrt{\left(1-\beta^2\right)^2+(2\xi\beta)^2}}\times\frac{P_0}{k}-\frac{P_0}{k\alpha} \tag{70}$$

or

$$-\frac{P_0}{k\alpha}-\sqrt{1-\frac{(2\xi\beta)^2}{\left(1-\beta^2\right)^2+(2\xi\beta)^2}}\times\frac{P_0}{k}\le\Delta_1\le\sqrt{1-\frac{(2\xi\beta)^2}{\left(1-\beta^2\right)^2+(2\xi\beta)^2}}\times\frac{P_0}{k}-\frac{P_0}{k\alpha} \tag{71}$$

So, the upper and lower limits of velocity deviation (Δ_1) were determined using Eqn. (71). Velocity deviation does not occur before reaching the vertical axis when the direction of motion is clockwise. So, the positive part of the sine function between zero to (+1) is considered as the possible zone for velocity deviation and by assuming the deviation greater than zero, the Eqn. (71) is re-written as:

$$\overline{)0\le\Delta_1\le\frac{\left(1-\beta^2\right)}{\sqrt{\left(1-\beta^2\right)^2+(2\xi\beta)^2}}\times\frac{P_0}{k}-\frac{P_0}{k\alpha}} \tag{72}$$

However, practically the velocity deviation (Δ_1) may occur before the vertical reference axis ($\Delta_1 \le 0$). Fig. 4, illustrates the variation of velocity deviation (Δ_1) versus the frequency ratio.

(β) and the different force amplitude ratios (α) for a particular example when $P_0 = 200,000N$ and $k = 100,000N/m$.

The following findings were derived from Fig. 4:

1) The implementation of HDM led to a reduction in the velocity deviation and consequently, the MV of the excited system. The HDM installation reduced the velocity deviation between 3 % and 94 %.
2) A higher value of damping ratio (ξ) resulted in less velocity deviation. The effects of the damping ratio in reducing velocity deviation were more tangible for frequency ratios between 0.85 and 1.15.
3) In high frictions, the force amplitude ratio is reduced because friction controls the SDOF system response.
4) Based on the figures, the total range for velocity deviation was 4 for all force amplitude ratios (α):

- Force amplitude ratio (α) = 10 → Velocity Deviation Range: −2.2 ~ 1.8
- Force amplitude ratio (α) = 5 → Velocity Deviation Range: −2.4 ~ 1.6

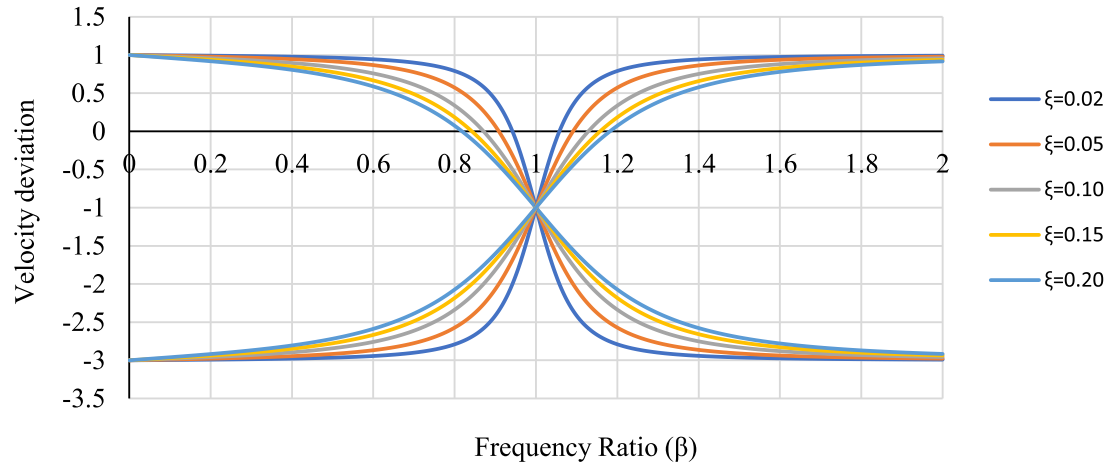

(a): Force amplitude ratio (α) = 2

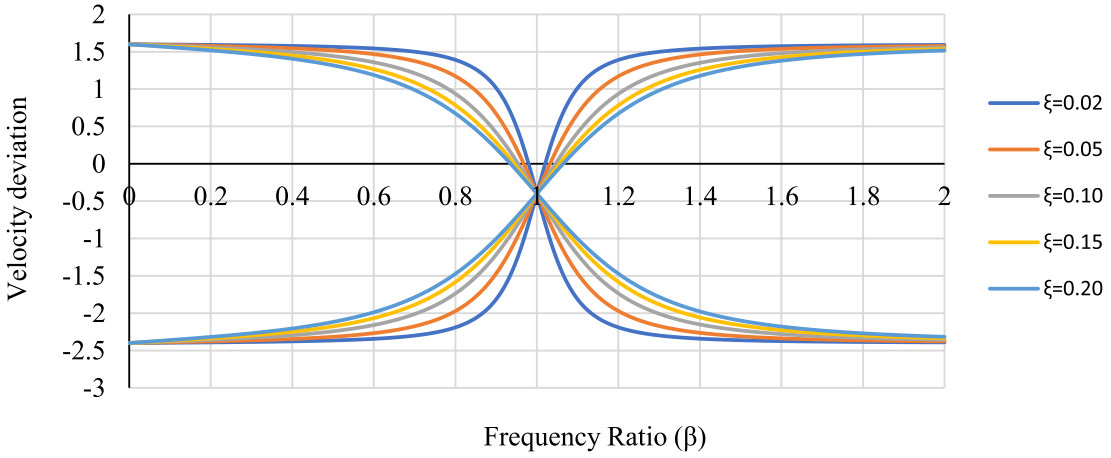

(b): Force amplitude ratio (α) = 5

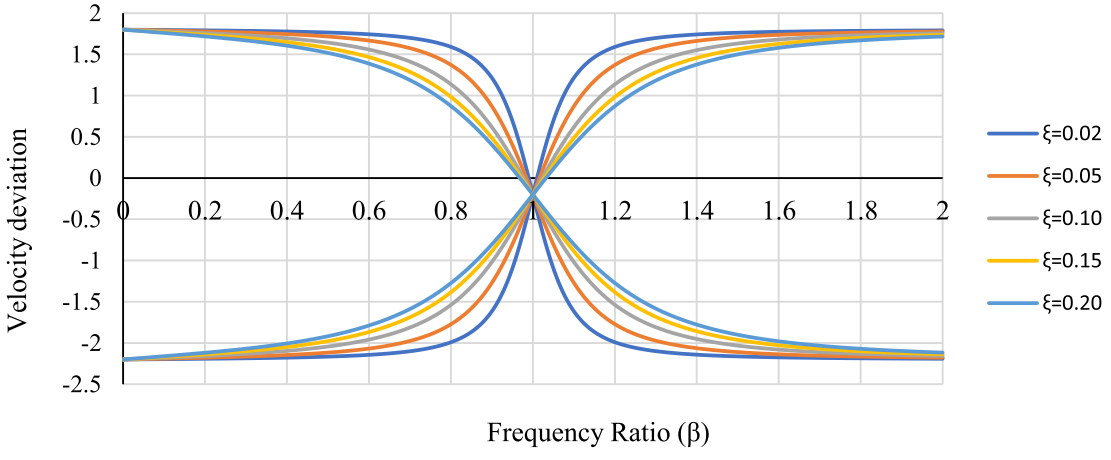

(c): Force amplitude ratio (α) = 10

Fig. 4. Velocity deviation for various amounts of the force amplitude ratio (α), frequency ratio (β) and hybrid damping ratio (ξ).

- Force amplitude ratio $(\alpha) = 2 \rightarrow$ Velocity Deviation Range: $-3.0 \sim 1.0$

Therefore, the total range of velocity deviation is the same for any force amplitude ratio. However, decreasing the force amplitude ratio (α) due to an increase in the friction, which will lead to a shift in the curves for velocity deviation (Δ_1) to the lower ranges.

5) All curves for different force amplitude and damping ratios pass through the same point at the frequency ratio (β), 1. Thus, it can be concluded that in the resonance, when the natural frequency of the structures is equal to the frequency of the external load, velocity deviation (Δ_1) is independent of the hybrid damping ratio (ξ). Although the movement of structure reduces via hybrid damping, MV is not affected by hybrid damping at the resonance point.
6) The intersection points for velocity deviation curves for the high force amplitude ratio (α) at the resonance point $(\beta = 1)$ was 0. However, when the force ratio decreases to 10 and below, the intersection point moved lower (to the negative side) from -0.2 at $\alpha = 10$ to -1 at the force amplitude ratio (α) of 1. Therefore, when the Coulomb friction is increased, the MV corresponding to the velocity deviation shifts far from the steady-state condition (position before movement). In low Coulomb frictions, the MV occurs in the steady-state point of the SDOF system (where displacement was 0 before excitation).

When the Coulomb friction is high, the point of MV occurrence shifts far from the steady-state point close to the point corresponding to the MD.

7) Similarly, by increasing the frequency ratio (β) beyond 1, the Coulomb friction force influences the velocity deviation (Δ_1) to become greater causing the MV to occur far from the steady point (position before movement).

4.2. Determining time lag of MV

The second main objective of this study is to determine the time at which the MV happens (t_1). To fulfil this purpose, Eqn. (60) is modified using trigonometric rules as illustrated below:

$$tan(\alpha+\beta) = \frac{tan\alpha + tan\beta}{1 - tan\alpha * tan\beta} \tag{73}$$

$$tan\left(\omega_n(t_2 - t_1) - \frac{\pi_1}{2}\right) = \frac{tan(\omega_n(t_2 - t_1)) - tan\left(\frac{\pi_1}{2}\right)}{1 + tan(\omega_n(t_2 - t_1)) * tan\left(\frac{\pi_1}{2}\right)} = \frac{a_1 - \xi b_1}{\xi a_1 + b_1} \tag{74}$$

Eqn. (74) was simplified to generate an equation for time lag:

$$tan(\omega_n(t_2 - t_1)) = \frac{\frac{a_1 - \xi b_1}{\xi a_1 + b_1}(1 + cos\pi_1) + sin\pi_1}{(1 + cos\pi_1) - \frac{a_1 - \xi b_1}{\xi a_1 + b_1} sin\pi_1} \tag{75}$$

Substituting a_1 and b_1 from Eqs. (65) and (66) into Eqn. (75), yields:

$$tan(\omega_n(t_2 - t_1)) = \frac{-\xi(1 + cos\pi_1) + sin\pi_1}{(1 + cos\pi_1) + \xi sin\pi_1} \tag{76}$$

The only unknown parameter in the Eqn. (76) was t_1, which can be estimated using any math software like MATLAB. By determining the time of MV (t_1), the MV deviation (Δ_1) from Eqn. (67) and subsequently the MV (V_0) from Eqn. (68) can be calculated. Since all the required parameters have been obtained, the behavior of HDM can be assessed under the external loads, whereby the responses of the system can be computed using the derived formulations.

5. Defining a borderline for force amplitude ratio to escape the sticking phase in HDM

The fundamental assumption in this study denotes that the oscillatory motion occurs in the non-sticking phase where all the aforementioned equations were derived for this condition. Thus, a criterion is required to ensure that the system's motion is taking place in the zero-duration sticking phase during the operation. To skip the sticking phase, it is rational to satisfy the following equation:

$$\left|P_0 sin\omega_f t - kx(t)\right| \geq f_d \tag{77}$$

Based on the nature of oscillation, the critical times to trap into the sticking phase can be t_2 or t_4, where the velocity becomes zero at these times and friction is applied to the SDOF system simultaneously to increase the possibility of non-zero-duration sticking. At the other points, as there are relatively high velocities and the kinetic energy exists in the system, the probability of occurring the sticking phase is zero. Hence, by rearranging Eqn. (77) for time t_2 could determine the boundary limits for the force amplitude ratio (α). The procedure is represented by the following equation:

$$\left|P_0 sin\omega_f t_2 - kx(t_2)\right| \geq f_d \tag{78}$$

By taking the boundary conditions with knowing that the structure displacement at point 2 is equal to the MD $(x(t_2) = +\Delta_0)$, introducing the sine function of time lag at point 2 $(sin\omega_f t_2)$ and the MD (Δ_0) from Eqs. (55) and (58) respectively, Eqn. (78) can be reshaped as:

$$\frac{k}{f_d}(\Delta_0) - \frac{P_0}{f_d A}\left(\Delta_0 - \frac{\xi B sin\pi_1}{1 + cos\pi_1}\right) = -1 \tag{79}$$

The simplified Eqn. (7) created the following equation:

$$\left(\frac{\alpha^2\beta^2}{\left(1-\beta^2\right)^2 + (2\xi\beta)^2} - \left(\frac{sin\pi_1}{1 + cos\pi_1}\right)^2\right)\left(1 - \sqrt{\left(1-\beta^2\right)^2 + (2\xi\beta)^2}\right)^2 = \left(\beta + \frac{\xi\beta sin\pi_1}{1 + cos\pi_1}\right)^2 \tag{80}$$

When the damping ratio (ξ) is equal to zero, Eqn. (80) is converted to Hong et al.'s equation for force amplitude ratio (α) and acts as a proof of the validity of the proposed formulas in this study. Finally, α appears in the form of:

$$\alpha \geq \sqrt{\frac{\left[\left(1-\beta^2\right)^2 + (2\xi\beta)^2\right]\left[\left(\beta + \frac{\xi\beta sin\pi_1}{1+cos\pi_1}\right)^2 + \left(1 - \sqrt{\left(1-\beta^2\right)^2 + (2\xi\beta)^2}\right)^2\left(\frac{sin\pi_1}{1+cos\pi_1}\right)^2\right]}{\left[\beta^2\left(1 - \sqrt{\left(1-\beta^2\right)^2 + (2\xi\beta)^2}\right)^2\right]}} \tag{81}$$

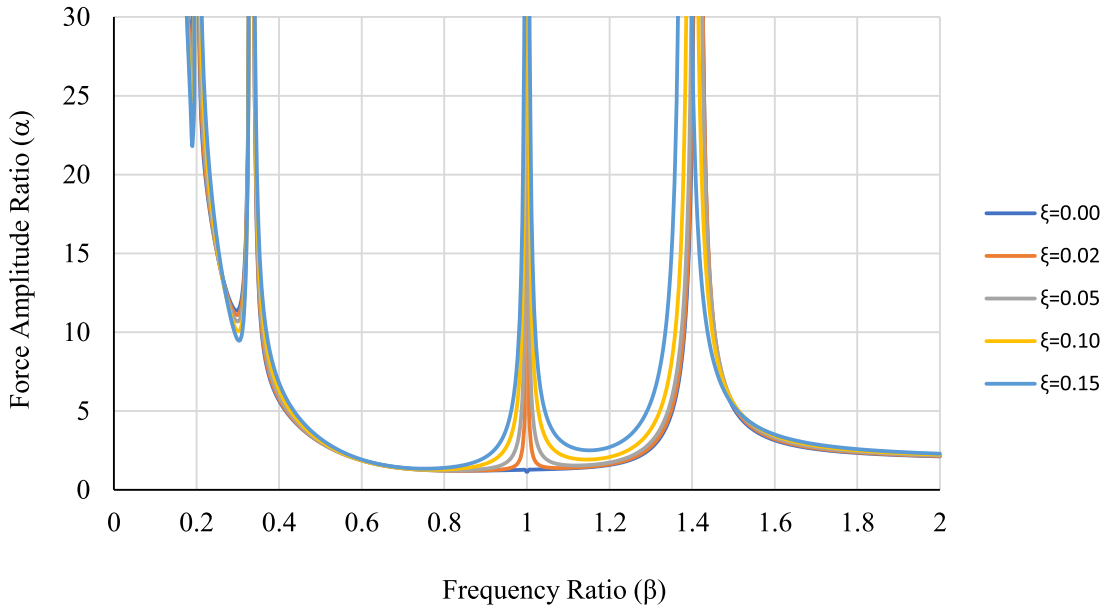

(a): Borderlines for force amplitude ratio (α)

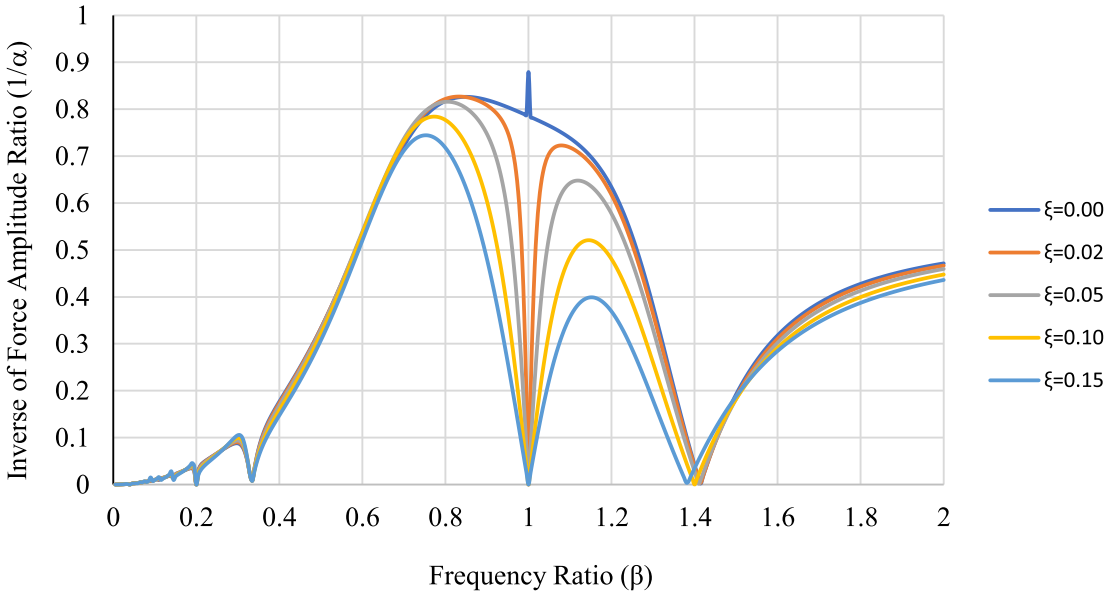

(b): Borderlines for the inverse of force amplitude ratio (1/α)

Fig. 5. Borderlines for force amplitude ratio (α) and the inverse of force amplitude ratio (1/α) versus frequency ratio (β).

or

$$\frac{1}{\alpha} \leq \sqrt{\frac{\left[\beta^2\left(1-\sqrt{(1-\beta^2)^2+(2\xi\beta)^2}\right)^2\right]}{\left[(1-\beta^2)^2+(2\xi\beta)^2\right]\left[\left(\beta+\frac{\xi\beta sin\pi_1}{1+cos\pi_1}\right)^2+\left(1-\sqrt{(1-\beta^2)^2+(2\xi\beta)^2}\right)^2\left(\frac{sin\pi_1}{1+cos\pi_1}\right)^2\right]}} \tag{82}$$

Eqn. (81) revealed that the force amplitude ratio (α) depends on the damping and frequency ratios. Therefore, its relevant graphs can be depicted and the appropriate amounts for the force amplitude ratio (α) to avoid the sticking phase in the dynamic motion of the hybridized systems can be selected according to them. Fig. 5 illustrates the borderlines for the force amplitude ratio (α) and its inverse ($1/\alpha$) versus

different frequency ratios (β).

The areas above the curves in Fig. 5-(a) and under the graphs in Fig. 5-(b) are the desired design domains for the force amplitude ratio (α) and the inverse of the force amplitude ratio ($1/\alpha$), respectively.

These criteria can be used as a guideline for structural designers to avoid the sticking phase in finding the steady-state response of motion for the oscillatory systems with Coulomb friction.

Fig. 5 revealed that the force amplitude ratio (α) was almost greater than 1.13, when the resonance occurred at a frequency ratio (β) close to 1 and the SDOF system experienced MD under applied excitation.

Contrarily, when the force amplitude ratio (α) was low (lower than 1.13 in this example), the sticking phase occurred and the structure did not oscillate. Therefore, it can be concluded that the sticking phase could occur under resonance conditions if the amplitude of the external loading is not adequate to overcome Coulomb friction.

Based on the results, the implementation of HDM with high damping ability can result in the sticking condition representative of an over damping status in the system. Therefore, employing HDM in the system with Coulomb friction is necessary to be processed carefully to avoid the sticking phase in a (β) range close to 1 and ineffective proposed damping solution with the hybridized damping mechanism.

6. Privileges of developed method to determine the Steady-State response of structure with HDS

The privileges of the developed method to determine the steady-state response of the structure compared to similar prior art available in the literature are summarized as follows:

- In the proposed method, the supplementary viscous damping in addition to the inherent damping was considered an HDS in the focused schematic model.
- Generally, the governor equation of motion for MDOF systems is uncoupled by assuming the inherent damping ratio to be proportional to the mass and stiffness (similar to Rayleigh). However, the developed method in this study revealed that steady-state solution of extended MDOF systems can be derived without having any specific assumption or constraint for damping.
- This study employed a direct formulation to derive structural responses for the proposed hybrid system to effectively reduce computation time and effort.
- The proposed method is a pioneer in investigating the simple formulation derived for MD and its corresponding time for the SDOF equipped with the viscous damper in presence of Coulomb friction.
- The proposed hybrid system in the present study is applicable as a hybrid TMD in the structures. However, there is no possibility of such applications being considered in the MDOF systems.

7. Conclusion

In the present study, the HDM which is the combination of the Coulomb friction and viscous damper was introduced to the SDOF system subjected to harmonic vibration to dissipate the effects of applied vibrations. Accordingly, the steady-state response of the proposed system was formulated by embedding the effects of hybrid damping in the equation of motions and the corresponding equations for MD, MV deviation, and time lag were derived.

The results proved that the implementation of HDM in the SDOF system can significantly contribute to diminishing DAF in the range of 5 % to 98 % for various frequencies and force amplitude ratios. As for the frequency ratio (β) in the range of 0 to 0.6, the force amplitude ratio (α) was more effective for the variations of DAF compared to the harmonic hybrid damping ratio (ξ) which had no effects.

This study also demonstrated that DAF was equal to force amplitude in this range of frequency ratio (β).

While the effects of HDM are more tangible for frequency ratios (β) within 0.6 to 1.15, the hybrid damping ratio (ξ) reduced DAF noticeably in the range of 5 % to 98 %, especially for the frequencies close to resonance ($\beta = 1$).

Whereas, the frequency ratio (β) of more than 1.15 is known as the desirable design zone since DAF is minimized. So, an increase in the hybrid damping ratio (ξ) in this frequency range could lead to reduced displacement amplitude, while an increase in frequency ratio could minimize DAF.

On the other hand, the implementation of HDM resulted in the reduction of the velocity deviation and the MV of the exciting SDOF system in the range of 3 % to 94 % for various force amplitude ratio (α), frequency ratio (β) and hybrid damping ratio (ξ).

An increase in force amplitude ratio causes a higher velocity deviation, however, employing HDM compensates for the situation and returns the velocity deviation (Δ_1) back to its original state.

Thereafter, a borderline was formulated for the force amplitude ratio to avoid the sticking phase in the Coulomb friction since sticking complicates the analytical approach.

It is evident from the drawn borderline graphs that when the damping ratio rises, the force amplitude ratio must increase to avoid the system from entering the sticking phase. Therefore, it can be concluded that the addition of HDM to the SDOF acts as an additional friction force that leads the structure into the sticking phase. Therefore, the force amplitude ratio must be varied proportionally with the hybrid damping ratio to provide zero duration sticking points when the SDOF system oscillates.

The proposed hybridized SDOF system is also applicable as a Tuned Mass Damper (TMD) in the structures to increase their dynamic performance.

Declaration of Competing Interest

The authors declare that they have no known competing financial interests or personal relationships that could have appeared to influence the work reported in this paper.

References

[1] Minkin L, Sikes D. Measuring the coefficients of kinetic and rolling friction by exploring decaying mass-spring oscillations. Phys Educ 2018;53(1):015001.
[2] Feeny B, Guran AS, Hinrichs N, Popp K. A historical review on dry friction and stick-slip phenomena. 1998:321-41.
[3] Hong HK, Liu CS. Non-sticking oscillation formulae for Coulomb friction under harmonic loading. J Sound Vib 2001;244(5):883–98.
[4] Younis CJ, Tadjbakhsh IG. Response of sliding rigid structure to base excitation. J Eng Mech 1984;110(3):417–32.
[5] Lopez I, Busturia JM, Nijmeijer H. Energy dissipation of a friction damper. J Sound Vib 2004;278(3):539–61.
[6] Ferreira F, Moutinho C, Cunha Á, Caetano E. Use of semi-active tuned mass dampers to control footbridges subjected to synchronous lateral excitation. J Sound Vib 2019;446:176–94.
[7] Hartog JD. Forced vibrations with combined Coulomb and viscous friction. Trans Am Soc Mech Eng 1931;53:107–15.
[8] Hong HK, Liu CS. Coulomb friction oscillator: modelling and responses to harmonic loads and base excitations. J Sound Vib 2000;229(5):1171–92.
[9] Hundal MS. Response of a base excited system with Coulomb and viscous friction. J Sound Vib 1979;64(3):371–8.
[10] Beucke KE, Kelly JM. Equivalent linearizations for practical hysteretic systems. Int J Non Linear Mech 1985;20(4):211–38.
[11] Makris N, Constantinou MC. Analysis of motion resisted by friction. I. Constant coulomb and linear/coulomb friction*. Journal of Structural Mechanics 1991;19 (4):477–500.
[12] Pierre C, Ferri AA, Dowell EH. Multi-harmonic analysis of dry friction damped systems using an incremental harmonic balance method. J Appl Mech 1985;52(4): 958–64.
[13] Chen LY, Chen JT, Chen CH, Hong HK. Free vibration of a SDOF system with hysteretic damping. Mech Res Commun 1994;21(6):599–604.
[14] Nayfeh AH, Mook DT, Holmes P. Nonlinear oscillations. 1980.
[15] Cacciola P, Tombari A. Steady-state harmonic response of nonlinear soil-structure interaction problems through the Preisach formalism. Soil Dyn Earthquake Eng 2021;144:106669.
[16] Estakhraji SIZ, Allen MS. Extension of the Harmonic Balance Method for dynamic systems with Iwan joints. Mech Syst Sig Process 2022;166:108434.

[17] Riddoch DJ, Cicirello A, Hills DA. Response of a mass-spring system subject to Coulomb damping and harmonic base excitation. Int J Solids Struct 2020;193:527–34.
[18] Marino L, Cicirello A. Multi-degree-of-freedom systems with a Coulomb friction contact: analytical boundaries of motion regimes. Nonlinear Dyn 2021;104(1):35–63.
[19] Yadav OP, Vyas NS. Stick–slips and jerks in an SDOF system with dry friction and clearance. Int J Non Linear Mech 2021;137:103790.
[20] Marino L, Cicirello A. Coulomb friction effect on the forced vibration of damped mass–spring systems. J Sound Vib 2022;535:117085.